Energy Conversion. Vol. 16, pp. 111–123. Pergamon Press, 1977. Printed in Great Britain

SOLAR ENERGY AND THE STEAM RANKINE CYCLE FOR DRIVING AND ASSISTING HEAT PUMPS IN HEATING AND COOLING MODES

NOAM LIOR

Department of Mechanical Engineering and Applied Mechanics,
University of Pennsylvania, Philadelphia, PA 19174, U.S.A.

(*Received* 31 *March* 1976)

Abstract—Various methods for reducing the purchased, resource energy consumption of vapor-compression heat pumps in both heating and cooling modes are analyzed and compared to conventional systems. The results are presented in detailed system analysis curves for the relevant range of major design parameters. One of the methods studied is the application of a solar-powered, fuel-superheated Rankine cycle incorporating a steam turbine. This cycle would drive the heat pump in the cooling mode. Fuel-fired, it would drive the heat pump in the heating mode, with system performance augmented by utilizing the waste heat from the cycle, as well as by solar energy.

In the cooling mode, resource energy savings of 50–60% are obtained. In the heating mode, resource energy use is reduced 3 to 4 fold.

Heat pumps Solar energy Rankine cycles Solar heating and cooling Solar power Solar assisted heat pumps

INTRODUCTION

The fact that a part of the heat delivered to the building by a heat pump comes from cooling a "free" heat source such as outdoor air, water or soil, usually results in lower purchased resource energy consumption than that incurred by other, conventionally used systems for heating buildings (cf. [1–3]). The term "resource energy" used throughout this study defines the available energy of fuel before any subsequent energy conversion, and serves as an improved basis for comparing dissimilar forms of energy, such as electrical and thermal. For example, in considering electrical energy, the associated resource energy is that available in the original fuel used to produce that quantity of electrical energy, taking into consideration the losses of generation, transmission, and distribution.

Heat pumps are incorporated into a single system with year-around, pollution-free and safe operation. The present fuel shortage and the increasing cost of energy thus make heat pumps viable and possibly superior to other systems, particularly when *both* winter heating and summer cooling are needed. It is expected therefore that heat pumps will constitute an increasing portion of the heating and air conditioning equipment in use.

Further reductions in purchased energy consumption by heat pumps during the heating period are possible because of their ability to utilize low-temperature energy (at the evaporator coil) and convert it to higher temperature energy suitable for heating. Possible sources of low-temperature energy are the waste heat from power and processing plants, as well as heat generated by equipment and lighting directly in the building. Proper design and judicious utilization of such heat can result in substantial energy savings during the heating period [4, 5]. Another significant source of such energy is the sun.

Application of solar energy to augment the performance of heat pumps has been under consideration for a long time [6, 7], with actual installations achieving energy cost savings of 70–75% [8, 9]. Solar energy collected at sufficiently high temperatures, during periods of adequately high insolation and ambient temperature can be used to heat the building directly. When the ambient conditions cause the solar collector fluid to drop below *ca.* 35°C, the heat collected is used to heat the heat pump evaporator. Solar heat collection at lower collector temperatures is more efficient, or alternatively, the collection of the same amount of heat would require a collector which is either simpler of smaller, and thus less expensive.

An additional purchased-energy saving in the operation of the heat pump can be obtained by driving its compressor by a thermal engine, where the engine cycle fluid is heated by solar energy. A large variety of methods for the production of mechanical power from solar energy were proposed and demonstrated in the past [10–13]. While high collection temperatures result in better cycle efficiency, they require expensive solar concentrators which are also very sensitive to the intensity and direction of the solar radiation. Flat plate solar collectors provide lower collection temperatures, usually 80–110°C at most, but are cheaper and make use of both the diffuse and direct components of radiation. Resulting from extensive performance studies of flat plate solar collectors [14],

two of the most viable designs are considered here: a double-glazed collector with a flat-black absorber, and a single-glazed collector with a selective-black absorber. For driving air conditioners or heat pumps, some of the most promising power generation schemes at present utilize Rankine cycles employing reciprocating engines [15], rotary engines [16, 17], and turbines [18–22].

Comparatively, turbines exhibit simple construction, small friction losses, no lubricant required in cycle fluid, low maintenance and high reliability, low noise and vibrations, easy regulation, and small size with large expansion to condenser pressure and temperature. Their major disadvantages are that presently available off-the-shelf small turbines have low efficiency (below 50%), and somewhat higher cost. Initial specific studies on small turbines driven by low temperature solar energy have emphasized low turbine cost without too much concern for efficiency [23, 24]. More recently, high efficiency (70–80% isentropic) units using organic fluids have been built and operated [19, 21, 22], and a steam turbine of similar efficiency was being developed [20]. Proper design and mass production techniques seem to be at present at the point where cost of such high-efficiency turbines can be reduced sufficiently to compete very favorably with other types of engines. Based on the preliminary results [16], the rotary engine seems also to have significant potential for application in such systems, particularly for smaller size units.

While organic fluids in Rankine cycles have some advantages over water, such as higher molecular weight and possibly positive slopes of temperature vs entropy at the vapor–mixture saturation line, they also may have serious disadvantages, such as instability, toxicity, flammability, low thermal conductivity, corrosiveness and higher cost. They also have low specific energy and usually cannot be easily superheated to increase the potential enthalpy drop between prespecified pressure limits. Superheating the relatively low-temperature steam emerging from the solar collector by another source of energy, such as a fuel-fired superheater, would increase the cycle efficiency with relatively small consumption of fuel, as proposed by Tabor [25] and others [20, 26], and as analyzed and conceptually developed by the author [27]. Also, the development of small steam turbines can draw upon the larger amount of experience available with this type of turbine, as compared to organic–fluid Rankine cycles which are to some extent still in the exploratory stage.

During the heating season, the application of a thermal engine to drive the heat pump has the added advantage of being able to utilize its waste heat (jacket cooling and exhaust) to augment the output of the heat pump, either by applying the energy directly to the building or to the heat-pump evaporator.

So far, most of the research effort in solar comfort cooling and refrigeration has been directed to absorption systems [9, 28–30]. The consistently low coefficients of performance obtained with such units and the predominance of the more efficient vapor compression units in the present market, indicates that vapor compression heat pumps may be a viable alternative to absorption systems.

The application of thermal storage and of operational policies varying from off-peak to continuous operation reduces the purchased-energy consumption further, makes it possible to use a smaller heat pump and levels the load both on the heat pump and the utility. Load leveling reduces energy-wasteful transients as well as utility load peaking, which is costly and results in power shortages, particularly during peak hot weather periods. Recent studies [31] of air conditioning combined with low temperature thermal storage show that a reduction of 50% in compressor size and in peak power requirement, and 6% in total energy use is obtained for a continuously operating system, as compared to conventional air conditioning systems. High temperature storage is needed for the heating period and for the operation of the solar-powered thermal engine (when applicable).

The following study concerns itself primarily with energy savings in several systems. A decision on choosing the best system would be based also on a cost analysis as well as on social and other considerations.

THE SOLAR STEAM TURBINE

The combined solar-powered, fuel-superheated (SPFS) Rankine cycle heat pump is shown in Fig. 1. The Rankine cycle employs superheat by external fuel, a regenerator and an economizer.

The description of the cycle on the enthalpy-entropy Mollier diagram is shown in Fig. 2.

Some of the major results of the interactively computerized thermodynamic analysis are displayed in Figs. 3–5. Terms not defined in the text and assumed values of parameters are given in the Nomenclature at the end of the paper. The major conclusions of the analysis are:

(A). The cycle efficiency η_{pc} increases almost linearly with the isentropic efficiency of the turbine, η_T. For example, a high efficiency turbine with $\eta_T = 75\%$, results in system performance improvement of 70% at 0°C superheat, and 56% at 550°C superheat, over an off-the-shelf small turbine which usually has a maximal efficiency of 45% in this range (for 98°C collector temperature, 37°C condenser).

(B). Also as expected, superheat improves the cycle efficiency. Under the same conditions, η_{pc} of the turbine with 75% isentropic efficiency is 76% larger when the steam is superheated by 550°C than for the case of no superheat, this by adding only *ca.* 23% non-solar energy (the superheater fuel).

Since wet steam is damaging to the turbine and lowers its performance significantly, the degree of minimal superheat necessary to have a "dry" turbine has been calculated and is shown in Fig. 4. For the

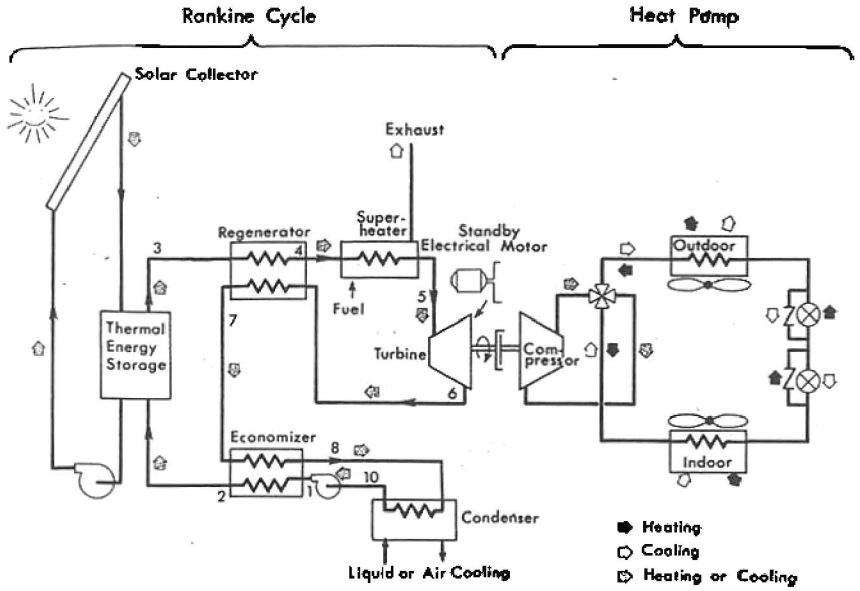

Fig. 1. Solar-powered, fuel-superheated (SPFS) steam Rankine cycle driven heat pump: system diagram.

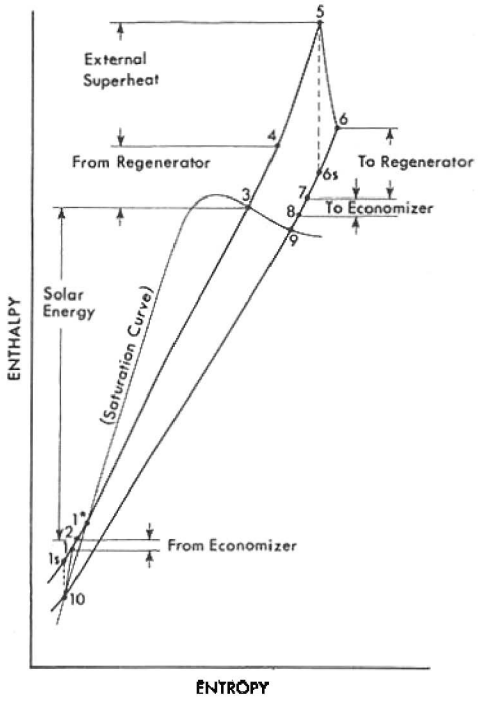

Fig. 2. Solar powered, fuel-superheated (SPFS) Rankine cycle Mollier diagram.

above case it amounts to 120°C, and it improves the cycle efficiency by 7% with the requirement of *ca.* 8% external fuel energy. Since the energy added to the superheater is compensated here by similar improvement in performance, it may even be beneficial to superheat the turbine at least sufficiently to reach dry exhaust conditions, in order to achieve longer life and higher reliability. Higher superheats would provide even higher benefits in system performance.

(C) A lower condensation temperature that could be achieved by improved methods for condenser cooling, improves the cycle efficiency by 15% when reducing the condensing temperature from 47 to 37°C for the above example with 550°C superheat. At the same time, the fuel ratio increases by 8%. Most noteworthy from observation of Figs. 4 and 5 is the fact that the efficiency of the proposed solar Rankine steam cycle with fuel-fired superheat is approximately twice that of the presently existing organic Rankine cycles which use no superheat, with a fuel consumption of only 20% of the total energy used.

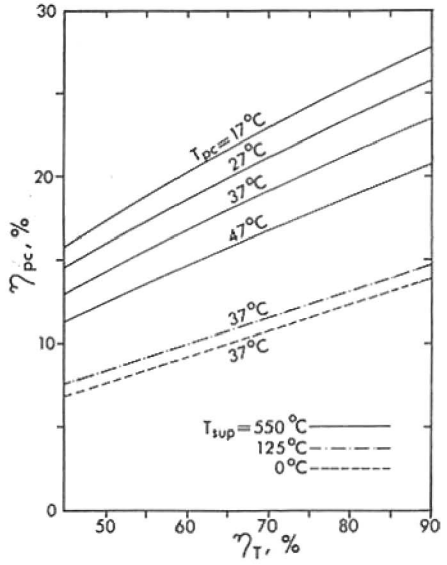

Fig. 3. SPFS Rankine cycle efficiency η_{pc} as a function of turbine isentropic efficiency η_T. T_{sc} = 98°C.

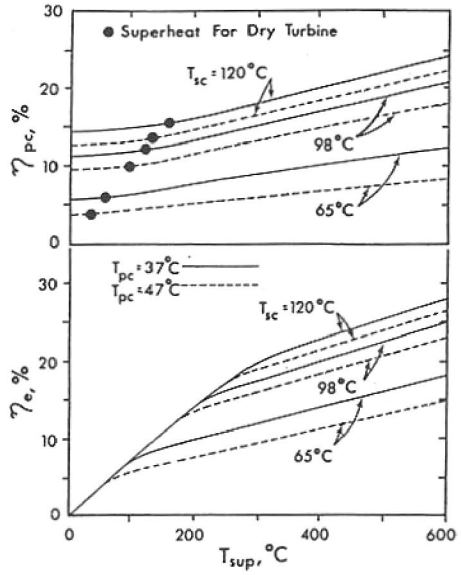

Fig. 4. SPFS Rankine cycle efficiency η_{pc} and fuel ratio η_e as a function of superheat T_{sup}, for various solar collector temperatures (T_{sc}) and condensing temperatures (T_{pc}). $\eta_T = 75\%$.

THE COOLING MODE

Solar energy utilization for summer cooling is particularly attractive due to the coincidence of high insolation and ambient temperature with high cooling load. Heat flow in the solar Rankine cycle-heat pump system during the cooling period is shown in Fig. 6. As mentioned previously, cold storage is proposed to be utilized to improve the performance of the system and decrease the size of the compressor. In locations where sufficient differences exist between day and night temperatures, with clear night sky, the solar collectors may be used to dissipate overnight the condenser heat of the heat pump and power cycle that was accumulated during the day. This makes possible the creation of a heat sink which is at lower temperature than the daily ambient, thus improving the performance of both heat pump and power cycle.

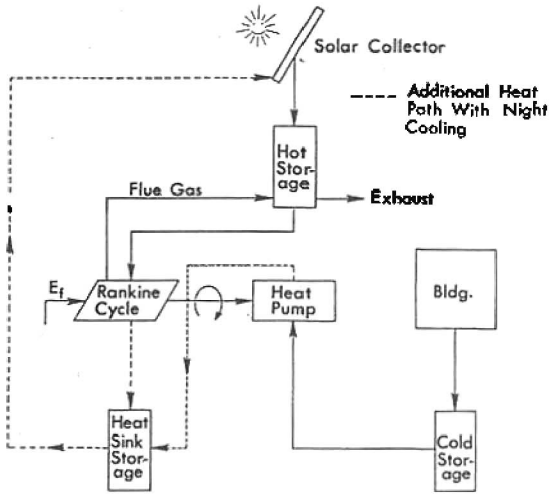

Fig. 6. Heat flow diagram of SPFS steam turbine driven heat pump system during cooling period.

To calculate the performance of the system, the Coefficient-of-Performance of the heat pump, as well as the relations between the temperatures of the heat pump condenser, evaporator, outside ambient and inside of cooled space were modeled after the recommendations in the ASHRAE Handbook [32]:

$$(\mathrm{COP})_c = 0.5\left(\frac{T_e + 273.15}{T_{c0} - T_e}\right) \tag{1}$$

$$T_{c0} = 21.8 + 0.76T_a \tag{2}$$

$$T_e = T_{bc} + 0.14T_a - 21.4. \tag{3}$$

The temperature of the air conditioned space, T_{bc}, was taken to be 78°F (25.6°C). Figures 7 and 8 show

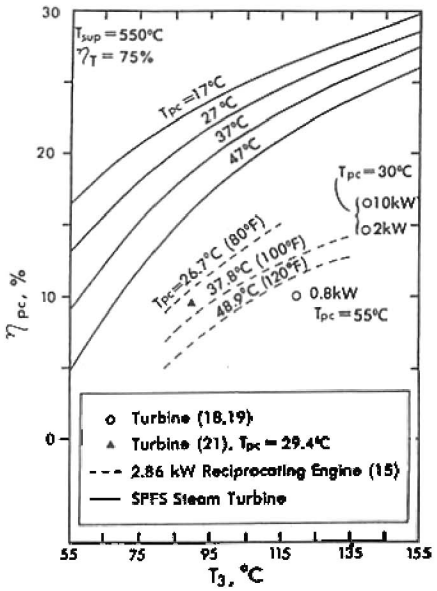

Fig. 5. SPFS Rankine cycle efficiency η_{pc} as a function of solar collector temperature, compared to existing organic fluid Rankine cycle systems.

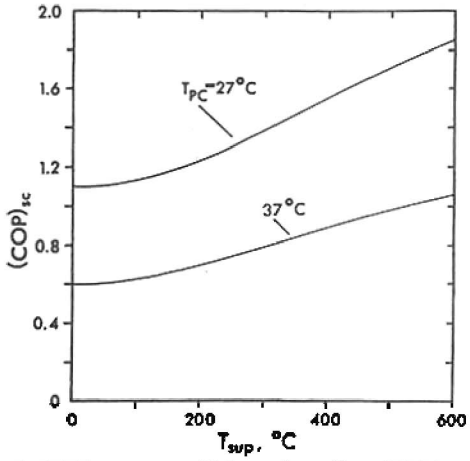

Fig. 7. SPFS system coefficient of cooling, $(\mathrm{COP})_{sc}$, as a function of superheat, T_{sup}, $\eta_T = 75\%$.

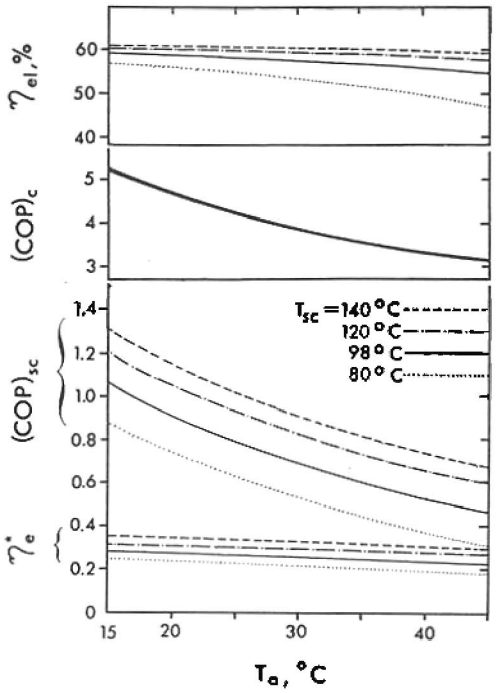

Fig. 8. Cooling system performance.

the system coefficient of performance for cooling, $(COP)_{sc}$ (still excluding any consideration of solar collector efficiency), as a function of superheat T_{sup} and ambient temperature T_a, respectively. Particularly noteworthy is the fact that the effect of reducing the condensing temperature on the $(COP)_{sc}$ is much larger than that on the η_{pc}. This results from the influence of T_{pc} on both power cycle *and* heat pump performance. For example, decreasing T_{pc} from 37 to 27°C for $T_{sc} = 98$°C and $T_{sup} = 550$°C, increases $(COP)_{sc}$ by 74%. The practical fuel ratio η_e^* takes into account the non-ideal efficiency of the superheater, η_{sup}, assumed here to be 85%. Figure 8 also shows η_{el}, the percentile resource energy saving, as compared to a conventional electric drive.

$$\eta_{el} = \frac{\{1/[0.3(COP)_c]\} - \{E_f/[(E_f + E_s)\eta_{pc}(COP)_c]\}}{1/0.3(COP)_c} \cdot 100$$

$$= \left[1 - \frac{0.3}{(1 + E_s/E_f)\eta_{pc}}\right] \cdot 100, \tag{4}$$

where the resource-energy efficiency of electrical power at the point of consumption is taken to be 30%. The obtained savings are close to 60%.

To analyze the performance of the total system, including solar collectors, the simplified formulas proposed by Hottel and Woertz [33] were used, with the coefficients extrapolated according to [34]. Thus, the efficiency of the solar collector is:

$$\eta_{sc} = \frac{E}{I}\left\{\overline{\alpha\tau} - \left[\frac{T_{sc} - T_a}{\dfrac{n}{C\left(\dfrac{T_{sc} - T_a}{n + f}\right)^{1/4}} + \dfrac{1}{h_w}}\right.\right.$$

$$\left.\left. + \frac{\sigma(T_{sc}^4 - T_a^4)}{\dfrac{1}{\epsilon} + \dfrac{2n + f - 1}{\epsilon_g} - n}\right]\right\}. \tag{5}$$

The total coefficient of performance of the system for cooling is therefore:

$$(COP)_{cs,tot} = \frac{E_W \cdot (COP)_c}{\left(\dfrac{E_s}{\eta_{sc}} + E_f\right)}, \tag{6}$$

where E_W is the turbine shaft work delivered to the heat pump.

To allow determination of the payback period relative to added system cost, a criterion, η_a, which determines the resource energy savings per square meter of solar collector area, was derived. The collector area has been chosen as the normalizing parameter due to the fact that it constitutes the major part of the cost of the system.

$$\eta_a = \eta_{sc} I\left[\frac{\eta_{pc}}{0.3} - \frac{E_f}{E_s}\left(1 - \frac{\eta_{pc}}{0.3}\right)\right]. \tag{7}$$

Finally, to be able to estimate the collector area needed for a specific application, this area per ton of cooling (3516.8 W), A, is computed:

$$A = \frac{3516.8}{(E_f/E_s + 1)(COP)_{sc}\eta_{sc} I}. \tag{8}$$

The major results for a double-glazed, flat black collector and a single-glazed selective black collector are presented in Figs. 9–11. η_{el} asymptotically flattens out at superheats above *ca.* 350°C. The single-glazed selective black collector is shown to perform better than the double-glazed flat-black one.

Increasing the temperature of the collector improves the efficiency of the power cycle, but it decreases the efficiency of the solar collector. This behavior is expressed in the maxima of the performance curves shown in Fig. 9. The maxima for the double-glazed collector are for about $85 \le T_{sc} \le 100$°C and for the single-glazed somewhat higher, $95 \le T_{sc} \le 115$.

THE HEATING MODE

Some of the major schemes for heating, outlined in Fig. 12, are described and compared. For the comparison of resource energy consumption by the various schemes, the heat load was calculated using the degree-day method. The method is probably not accurate enough for actual HVAC design, but can be useful for comparative purposes. The hourly heating load E_l is

$$E_l = \frac{E_d(65 - T_a)}{(T_{bh} - T_{ad})}, \tag{9}$$

where E_d is the hourly load under design conditions, T_a the average ambient temperature maintained in the

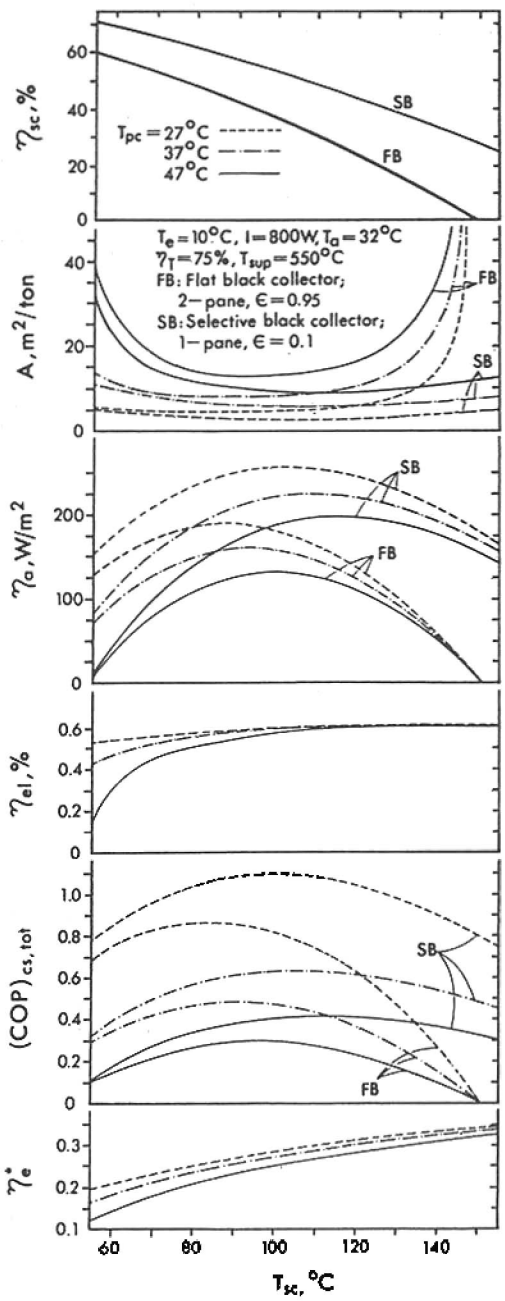

Fig. 9. Total system performance as a function of solar collector temperature.

building by the heating system (chosen here to be 21°C), and T_{ad} the ambient temperature at the design point. Since the example in Section 5 considers a building in Manhattan, New York, $T_{ad} = -10$°C. The temperatures in equation (9) are all in °F.

To perform a preliminary, building-independent analysis, equation (9) can be rewritten as

$$E_I = C_b(65 - T_a) = C_b \Delta T, \tag{10}$$

where

$$C_b \equiv \frac{E_d}{(T_{bh} - T_{ad})} \tag{11}$$

and

$$\Delta T \equiv 65 - T_a. \tag{12}$$

Referring to the system numbers in Fig. 12, the analysis follows:

Electric resistance heating

The resource energy required, E is simply

$$E = \frac{C_b \Delta T}{0.3} \tag{13}$$

and the specific, building-independent, resource energy E_H is

$$E_H = \frac{E}{C_b} = \frac{\Delta T}{0.3}, \tag{14}$$

shown as line A in Fig. 13.

Fuel-fired heating

The efficiency of the furnace is taken to be 60%. Thus,

$$E_H = \frac{\Delta T}{0.6}. \tag{15}$$

Electric-driven heat pump, with auxiliary electric resistance heaters

Up to the design point, the resistance heaters are not in operation and thus,

$$E_H = \frac{\Delta T}{0.3(\mathrm{COP})_H}, \tag{16}$$

where $(\mathrm{COP})_H$ is the coefficient of performance of the heat pump, for heating. Based on the recommendation in the ASHRAE Handbook [32], $(\mathrm{COP})_H$ can be estimated as

$$(\mathrm{COP})_H = 0.5 \frac{T_{co} + 273.15}{T_{co} - T_e}. \tag{17}$$

Equation (17) does not, however, seem to take the detrimental effect of evaporator-defrosting into account, and it has been corrected here on the basis of heat pump manufacturers' catalog data. The smooth solid and dashed line for $(\mathrm{COP})_H$ in Fig. 13 is based on equation (17), while the solid line contains the correction for defrosting.

Also from the ASHRAE Handbook [32]

$$T_{co} = T_{bh} + 0.671\, T_a + 21.34 \tag{18}$$

$$T_e = 0.743\, T_a - 9.57. \tag{19}$$

For temperatures below the design point, electrical resistance heaters augment the heating and,

$$E_H = \left\{ \frac{\Delta T_d [1 - (\mathrm{COP})_H]}{(\mathrm{COP})_{Hd}} + \Delta T \right\} \Big/ 0.3. \tag{20}$$

Equations (16) and (20) are shown as line C in Fig. 13. The dashed line C_1 represents the heat pump performance without defrosting or electric resistance heaters.

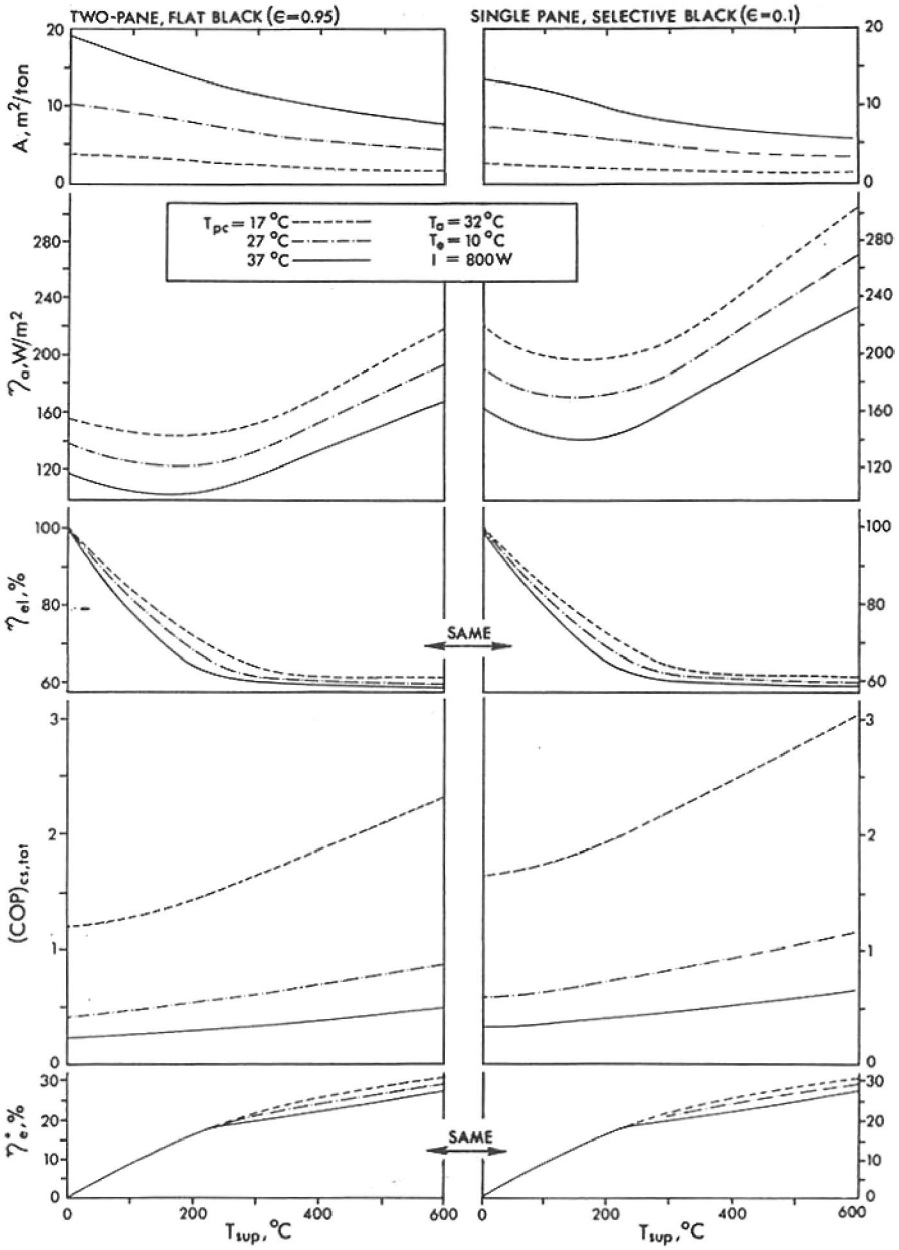

Fig. 10. Total system performance as a function of superheat.

Entirely solar heating

The specific solar collector area A_H, needed to satisfy the entire heat load is shown in Fig. 13. The collector temperature is 37°C, possibly the lowest practicably acceptable. Using equation (5) for η_{sc}

$$A_H = \frac{A}{C_b} = \frac{\Delta T}{\eta_{sc} I}, \tag{21}$$

where A is the total required collector area.

As shall also be discussed, heating entirely by solar means requires prohibitively large collector areas. The areas calculated here serve, however, as a good basis for comparison and as an upper limit which is of interest in the design of such systems.

Fuel-assisted solar heating

This is the most popular scheme contemplated at present (cf. [35, 36]).

$$E_H = \frac{\Delta T - A_H I \eta_{sc}}{0.6}. \tag{22}$$

For $I = 500\ \mathrm{W/m^2}$ and $T_{sc} = 37°\mathrm{C}$, E_H was investigated for collector areas of 5 and 25% from that required at the design temperature of $-10°\mathrm{C}$. From Fig. 13:

$$0.05 A_{Hd} = 0.00602 \frac{\mathrm{m^2}}{\mathrm{W/°C}}$$

and

$$0.25 A_{Hd} = 0.031 \frac{\mathrm{m^2}}{\mathrm{W/°C}}.$$

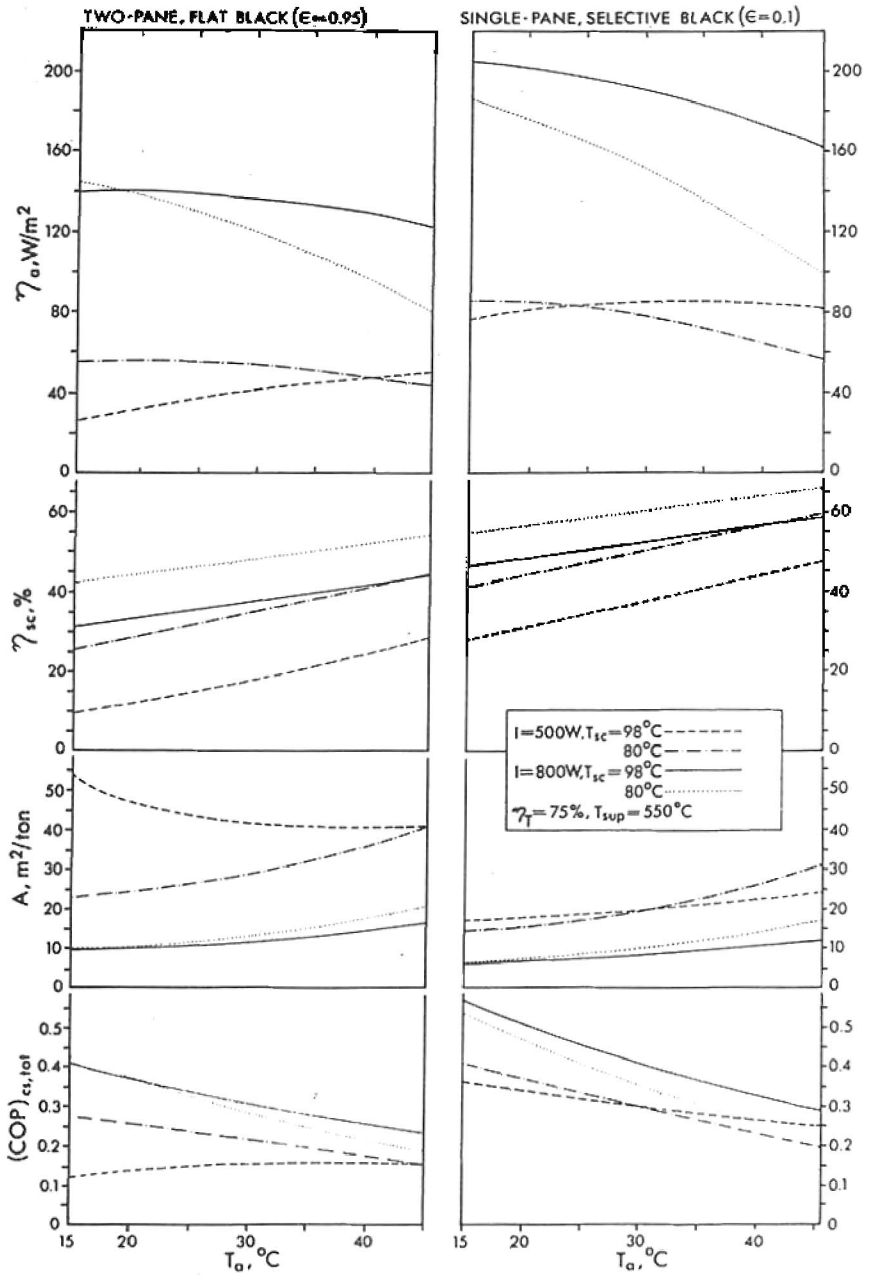

Fig. 11. Total system performance as a function of ambient temperature.

E_H for the 5 and 25% collector areas are shown as lines K and L, respectively, in Fig. 13.

Electric-driven heat pump with solar heating

Here, the building is heated partially by the heat pump and partially by solar collectors. Down to the design point,

$$E_H = \frac{\Delta T - A_H I \eta_{sc}}{0.3(\mathrm{COP})_H}. \tag{23}$$

For temperatures below the design point, electrical resistance heaters augment the performance of the heat pump, and

$$E_H = \frac{\Delta T + \dfrac{\Delta T_d}{(\mathrm{COP})_{Hd}}(1 - (\mathrm{COP})_H)}{0.3} - \frac{A_H I\left[\eta_{sc} + \dfrac{\eta_{scd}}{(\mathrm{COP})_{Hd}}(1 - (\mathrm{COP})_H)\right]}{0.3}. \tag{24}$$

Curve D shows E_H for 0.05 A_{Hd}, and curve H shows E_H for 0.25 A_{Hd}.

Electric-driven heat pump with solar assistance to evaporator

Applying solar heat to the heat pump evaporator has two principal advantages: It makes lower tem-

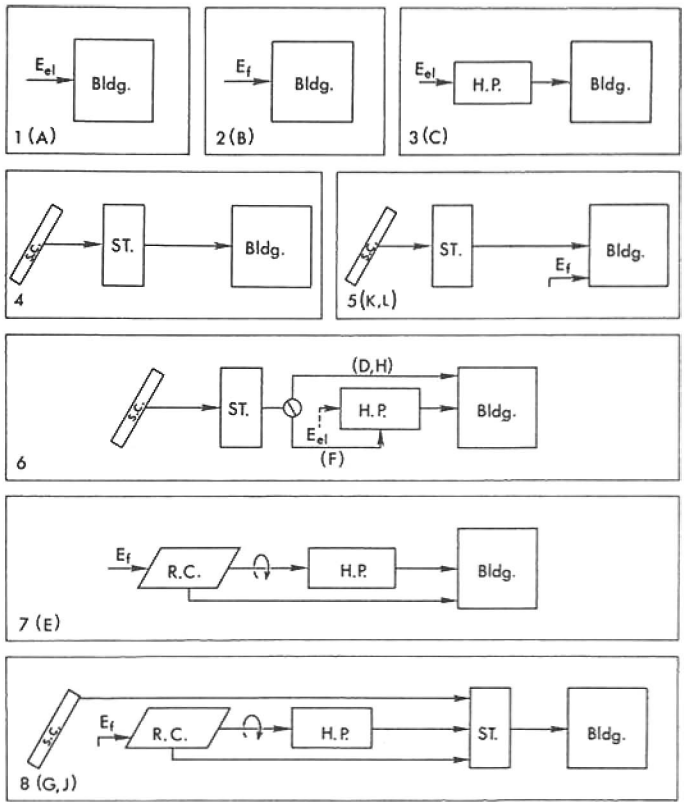

Fig. 12. Heating schemes analyzed in this study. (ST.: Thermal Storage; H.P.: Heat Pump; R.C.: Rankine Cycle).

perature solar collector operation possible, thus improving its efficiency, and improves the performance of the heat pump by increasing its $(COP)_H$ at low ambient temperatures, by eliminating frosting of the evaporator (when the temperature is maintained above freezing) and by stabilizing its operation through the maintenance of a constant evaporator temperature. While the analysis shows that in general the application of solar heat directly to the building is more efficient, it is possible that the solar heated fluid should be switched to the heat pump evaporator when ambient conditions do not provide for efficient direct solar heating (cf. [3]). Heating the evaporator at a lower temperature, the same collector area provided for direct heating at a higher temperature may be sufficient to maintain the evaporator ambient above freezing.

E_H is calculated by equations (16) and (20) with $(COP)_H = (COP)_{Hd} = 3.2$ for $T_a = 12°C$. It is shown as curve F in Fig. 13.

The specific collector area required in this case can be easily seen to be

$$A_H = \frac{\Delta T[1 - 1/(COP)_H]}{I\eta_{sc}} \tag{25}$$

approximately half of that required for direct solar heating under the above conditions.

Fuel-fired Rankine-cycle driven heat pump

In this scheme, the Rankine cycle condenser discharges heat to the building, thus adding to the energy delivered by the heat pump. The exhaust gases are used to defrost the heat pump evaporator. The Rankine cycle used is the one described in the second Section, operating at $T_3 = 98°C$ and $T_{sup} = 550°C$, with $\eta_T = 75\%$ and resulting $\eta_{pc} = 18.5\%$. The combustion efficiency of the Rankine cycle boiler is taken as $\eta_c = 70\%$.

Down to the design temperature

$$E_H = \frac{\Delta T}{\eta_c[1 + \eta_{pc}((COP)_H - 1)]}. \tag{26}$$

Below the design temperature, the system is augmented by a fuel-fired furnace, and

$$E_H = \frac{\Delta T + \dfrac{\Delta T_d}{1 + \eta_{pc}((COP)_{Hd} - 1)} \left\{\dfrac{0.6}{\eta_c} - [1 + \eta_{pc}((COP)_H - 1)]\right\}}{0.6} \tag{27}$$

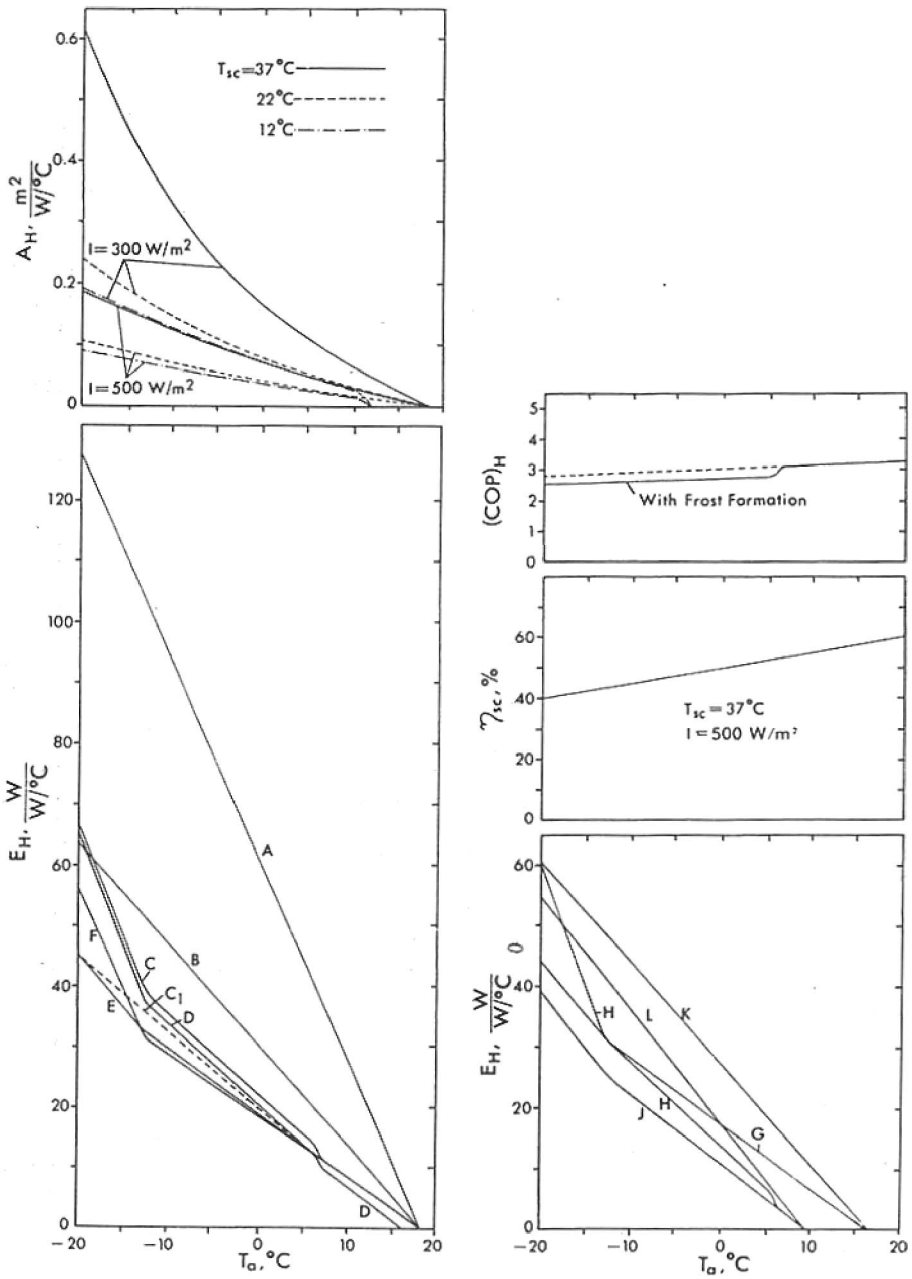

Fig. 13. Total system performance for heating. The solar collector is 2-pane, flat-black.

Equations (26) and (27) are displayed as curve E in Fig. 13.

Fuel-fired Rankine-cycle driven heat pump with solar heating

The same Rankine cycle proposed in the second Section and analyzed for solar cooling, can be used for heating. In most geographic locations it would, however, be more effective to use the existing solar collectors to heat the building directly, assisting their performance with the fuel-fired Rankine-cycle driven heat pump.

Down to the design temperature,

$$E_H = \frac{\Delta T - A_H I \eta_{sc}}{\eta_c \eta_{pc}[(\mathrm{COP})_H - 1] + 1}. \tag{28}$$

Below the design point, the system is augmented by a fuel-fired furnace, and

$$E_H = \frac{1}{0.6}\left\{\Delta T + \frac{\Delta T_d - A_H I \eta_{scd}}{1 + \eta_{pc}[(\mathrm{COP})_{Hd} - 1]} \times \left[\frac{0.6}{\eta_c} - 1 - \eta_{pc}((\mathrm{COP})_H - 1)\right] - A_H I \eta_{sc}\right\}. \tag{29}$$

Curve G shows E_H for $0.05A_{Hd}$, and curve J shows E_H for $0.25A_{Hd}$.

Table 1. Monthly and annual resource energy consumption for heating, in 10^2 MW-h 30-story office building in New York

Heating system	Fuel	Fuel + 5% solar	Heat pump	Rankine cycle heat pump	Heat pump + 5% solar	Solar-assisted heat pump	Rankine cycle heat pump + 5% solar	Fuel + 25% solar	Heat pump + 25% solar	Rankine cycle heat pump + 25% solar
Fig. 13 Curve	B	K	C	E	D	F	G	L	H	K
Sep	0.52	0.33	0.30	0.30	0.20	0.30	0.20	0.02	0.01	0.01
Oct	3.02	2.29	1.87	1.81	1.45	1.81	1.38	0.41	0.32	0.25
Nov	7.56	6.47	5.09	4.68	4.37	4.67	3.93	2.42	1.91	1.46
Dec	13.29	12.13	9.54	8.36	8.67	8.29	7.44	6.83	5.36	4.17
Jan	15.67	14.52	11.44	9.88	10.55	9.77	8.94	9.00	7.06	5.53
Feb	12.52	11.46	9.03	7.89	8.22	7.83	7.04	6.52	5.14	3.99
Mar	11.62	10.44	8.20	7.29	7.32	7.26	6.38	5.18	4.10	3.14
Apr	5.55	4.59	3.59	3.41	2.99	3.41	2.77	1.18	0.92	0.70
May	1.90	1.35	1.13	1.11	0.82	1.11	0.81	0.12	0.09	0.07
Annual	71.66	63.57	50.19	44.73	44.59	44.44	38.88	31.68	24.90	19.33

A COMPARATIVE EXAMPLE OF RESOURCE ENERGY CONSUMPTION

The comparative analysis of resource-energy consumption is performed on a high-rise office building in Manhattan, New York. While the hourly weather, insolation and load data would be needed for design purposes, the example treated here utilizes the frequency of occurrence of temperatures during each month, as provided by the U.S. Air Force Manual [37]. The average insolation during daytime is taken to be 500 W/m^2. Since hour-by-hour calculations are not performed, the effect of energy storage is not considered.

The office building has 30 stories, floor area/story (= roof area) of 1860 m^2, height/story of 3.7 m, wall area of 20,100 m^2 and 30% window area. The heat transfer coefficients are (in W/m^2 K): $U_{roof} = 1.2$, $U_{wall} = 1.25$, $U_{window} = 6.4$, $U_{floor} = 0.5$. Occupancy is 5 days a week, 8 hr a day, by 3000 persons. Total ventilation is 71 m^3/s, reduced to 10% of this value for unoccupied periods. The temperature during occupied periods is maintained at 21°C, reduced to 15°C during unoccupied ones. It is assumed that 50% of the process and lighting heat is reusable. Based on this, C_b for the occupied period, $C_{bo} = 94.2$ kW/°C and for the period when it is vacant, $C_{bv} = 70.3$ kW/°C.

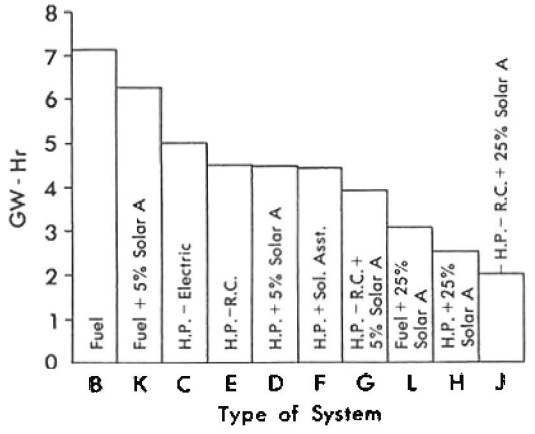

Fig. 14. Annual resource-energy Consumption for heating—30 story office building in New York (the letters on the abscissa correspond to the systems in Fig. 12. Abbreviations: H.P.: Heat Pump; R.C.: Rankine Cycle.)

The monthly and annual resource energy consumptions for the heating period are summarized in Table 1. The annual results are also displayed in Fig. 14. It can be seen that significant savings can be obtained by the application of solar energy and by the utilization of heat pumps and Rankine cycle drives.

Based on Fig. 13, and a C_b of 94 kW/°C, the collector area required for entire heating of the building, based on the design point of −10°C, is *ca.* 11,700 m^2. Assuming availability of solar radiation for 6 h and heat storage capacity of 3 days, the total required collector area would, as expected, be prohibitively large, in excess of 100,000 m^2. The foregoing calculations were therefore based on much smaller collector areas, compatible with available rooftop and wall space. The solar energy needs, therefore, to be augmented by an additional heat source always.

A simple approximation can be made of the compatibility of solar collector area requirements for cooling and heating. The design heating load of this building is 3 MW. Following [6], the cooling loading for the same building in the New York area would be *ca.* 2/3 of the heating load, i.e. 2 MW. From Fig. 11, it can be seen that the collector area required is *ca.* 5600 m^2, slightly larger than the area of one side of the building. Together with the available roof area, the building itself would be sufficient for mounting the collectors. Compared to the area needed for heating shown above, up to *ca.* 0.5 A_{fld} would thus be available for solar energy utilization.

CONCLUSIONS

A Rankine cycle utilizing solar energy as the primary source and superheated by an auxiliary fuel source has efficiencies which are about double that of comparable Rankine cycles without auxiliary superheat, this at the expense of only *ca.* 20–30% additional fuel energy. The cycle is well suited for driving vapor compression heat pumps for heating and cooling.

In cooling it offers a 50–60% resource energy saving as compared to a conventional electric-driven system. It is noteworthy that a recent study [38], found that the solar assisted Rankine cycle described here is also economically superior to other solar cooling systems.

As compared with conventional furnace heating, total resource energy consumption can be reduced 3 to 4 fold by employing partial solar heating assisted by a furnace, by a heat pump, or, best of all, by the Rankine-cycle driven heat pump.

Acknowledgement—The author wishes to thank Mr. T. A. V. Cassel for his assistance during the initial stages of the study, and Dr. J. C. Denton for his counsel and encouragement.

The study was partially supported by a grant from the National Science Foundation–RANN Program to the University of Pennsylvania National Center for Energy Management and Power.

NOMENCLATURE

(Including values of some of the parameters used in this study)

A	Solar collector area, in m^2, needed to provide one ton of cooling
A_H	Specific solar collector area for heating, equation (21)
c	$0.19 - 0.00078\beta$, in equation (5)
C_b	Equation (11)
$(COP)_c$	Heat pump coefficient of performance for cooling
$(COP)_H$	Heat pump coefficient of performance for heating
$(COP)_{sc}$	System coefficient of performance for cooling, excluding solar collector
$(COP)_{sc,tot}$	Overall system coefficient of performance for cooling, including solar collector efficiency
E	Resource energy, evaluated before conversion
E_{el}	Electrical energy
E_f	Fuel (combustion) energy ($= h_5$-h_4 for superheater)
E_H	E/C_b
E_s	Solar energy supplied to Rankine cycle ($= h_3$-h_2)
E_W	Shaft work delivered by turbine
f	0.76 for wind velocity of 10 m.p.h. in equation (5)
F	Solar collector efficiency factor, equation (15)
h	Enthalpy
h_w	Heat transfer coefficient on external surface of solar collector $= 1 + 0.3w$ (Btu/h ft^2F), in equation (5)
I	Insolation, W/m^2
n	Number of glass panes on collector
T_a	Ambient temperature
T_{bc}	Temperature of cooled space ($= 25.6°C$)
T_{bh}	Temperature of heated space ($= 21°C$)
T_{co}	Temperature of fluid in heat pump condenser
T_e	Temperature of fluid in heat pump evaporator
T_{pc}	Temperature of fluid in power-cycle condenser
T_{sc}	Temperature of fluid in solar collector
T_{sup}	Degrees of superheat
w	Wind velocity, m.p.h.
α	Absorptivity of solar collector absorber ($= 0.95$)
β	Angle of inclination of solar collector, degrees from horizontal ($= 45°$)
ΔT	Degree-day temperature difference $= 65 - T_a$ °F
ϵ	Emissivity of solar collector absorber ($= 0.95$ for flat-black, $= 0.1$ for selective black)
ϵ_g	Emissivity of solar collector glass ($= 0.88$)
η_a	Equation (7)
η_c	Combustion efficiency of the Rankine cycle boiler ($= 0.7$)
η_e	Fuel ratio $= \dfrac{E_f}{E_f + E_s}$
η_e^*	Practical fuel ratio $= \dfrac{E_f/\eta_{sup}}{(E_f/\eta_{sup}) + E_s}$
η_E	Efficiency of economizer ($=0.85$)
η_{el}	Equation (4)
η_m	Mechanical efficiency of turbine ($=0.98$)
η_p	Efficiency of pump in Rankine cycle ($=0.8$)
η_{pc}	Rankine cycle efficiency $= \dfrac{(h_5 - h_6)\eta_m}{h_5 - h_4 + (h_1 - h_{10}) + (h_3 - h_2)}$
η_R	Efficiency of regenerator ($= 0.85$)
η_{sc}	Solar collector efficiency
η_{sup}	Efficiency of superheater ($= 0.85$)
η_T	Isentropic efficiency of turbine
σ	The Stefan–Boltzman constant
τ	Transmittance of solar collector glass ($= 0.91$ single pane; $= 0.82$ double pane)

Subscripts d refers to load design conditions

REFERENCES

[1] E. R. Ambrose, *Heat Pumps and Electric Heating*, Wiley, NY (1966)

[2] R. L. Dunning, *Nuclear Energy Digest* (Westinghouse Electric Corp.) 4, 9 (1973).

[3] T. A. V. Cassel, H. G. Lorsch and N. Lior, *10th Intersociety Energy Conversion Engineering Conference*, Newark, DE (1975).

[4] R. T. Tamblyn, *Trans. ASHRAE*, Paper No. 1807, 51 (1963).

[5] R. A. Japhet, *Heating, Piping and Air Conditioning* 41, 89 (1969).

[6] R. C. Jordan and J. L. Threlkeld, *Heating, Piping and Air Conditioning* 26, 122 (1954).

[7] P. Sporn and E. R. Ambrose, in *Proc. World Symp. on Applied Solar Energy*, p. 159, Stanford Research Institute, Menlo Park, CA (1955).

[8] F. H. Bridgers, D. D. Paxton, and R. W. Haines, *Trans. ASHRAE* 64, 83 (1958).

[9] G. O. G. Löf, in *Introduction to the Utilization of solar Energy*, (Eds. A. M. Zarem and D. D. Erway,) Ch. 11. McGraw-Hill, NY (1963).

[10] J. I. Yellott, *Trans. ASME* 79, 1349 (1957).

[11] H. Tabor, *Solar Energy* 6, 89 (1962).

[12] R. C. Jordan, in *Introduction to the Utilization of Solar Energy*; (Eds. A. M. Zarem and D. D. Erway). Ch. 7 McGraw-Hill, NY (1963).

[13] C. R. Easton, R. W. Hallet, Jr., S. Gronich and R. L. Gervais, *9th Intersociety Energy Conversion Engineering Conference*, San Francisco, CA (1974).

[14] N. Lior and A. P. Saunders, Report No. NSF/RANN/SE/GI27976/TR731/1, University of Pennsylvania, PA (1974).
[15] S. L. Sargent and W. P. Teagan, *ASME Winter Conference*, Paper 73-WA/Sol-8, Detroit, MI (1963).
[16] S. E. Eckard, *10th Intersociety Energy Conversion Engineering Conference*, Newark, DE (1975).
[17] J. A. Eibling and D. M. Frieling, *Solar Energy* **17**, 313 (1975).
[18] H. Tabor and L. Y. Bronicki, *U.N. Conf. on New Sources of Energy*, Rome, Italy, Paper No. 35/5/S4 (1961).
[19] L. Y. Bronicki, *7th Intersociety Energy Conversion Engineering Conference*, San Diego, CA (1972).
[20] Energy Technology Inc., Cleveland, OH, *Private communication* (1973).
[21] D. Prigmore and R. Barber, *Solar Energy* **17**, 3, 185 (1975).
[22] F. R. Biancardi, M. D. Meader, W. A. Blecher and J. B. Hall, *10th Intersociety Energy Conversion Engineering Conference*, Newark, DE (1975).
[23] B. S. Leo and S. T. Hsu, *Solar Energy* **4**, 16 (1960).
[24] C. d'Amelio, *Solar Energy* **7**, 138 (1963).
[25] H. Tabor, *Bull. Res. Council of Israel* **5C**, 5 (1955).
[26] H. Heywood in *Solar Energy Research*, (Eds. F. Daniels and J. A. Duffie) 227 University of Wisconsin Press (1955).
[27] N. Lior, *9th Intersociety Energy Conversion Engineering Conference*, San Francisco, CA (1974).
[28] H. Tabor, *Solar Energy* **6**, 136 (1962).
[29] R. K. Swartman, *ASME Winter Meeting*, Paper 73-WA/Sol-6, Detroit MI (1973).
[30] P. Anderson, in *NSF/JPL Workshop Proceedings on Solar Cooling for Buildings*, Los Angeles, CA, (1974).
[31] S. I. Freedman, and J. C. Dudley, *7th Intersociety Energy Conversion Engineering Conference*, San Diego, CA.
[32] ASHRAE, Section V, Ch. 43 in *Guide and Data Book: Equipment*, American Society of Heating, Refrigerating and Air Conditioning Engineers, New York (1972).
[33] H. C. Hottel, and B. B. Woertz, *Trans. ASME* **64**, 91 (1942).
[34] G. O. G. Löf and R. A. Tybout, *ASME Winter Meeting*, Paper 72-WA/Sol-8, New York, N.Y. (1972).
[35] R. A. Tybout and G. O. G. Löf, *Nat. Res. J.* **10**, 268 (1970).
[36] H. G. Lorsch, *Energy Conversion* **13**, 1 (1973).
[37] U.S. Depts. of Air Force, Army and Navy, *Engineering Weather Data*, AFM 88-8, Ch. 6 (1967).
[38] H. M. Curran and M. Miller, *10th Intersociety Energy Conversion Engineering Conference*, Newark, DE (1975).